Ocean Engineering 264 (2022) 112499

Contents lists available at ScienceDirect

Ocean Engineering

journal homepage: www.elsevier.com/locate/oceaneng

Optimization of mooring line design parameters using Mooring Optimization Tool for FPSO (MooOpT4FPSO) with the consideration of integrated design methodology

Idris Ahmed Ja'e [a,b], Montasir Osman Ahmed Ali [a,*], Anurag Yenduri [c], Chiemela Victor Amaechi [d,e], Zafarullah Nizamani [f], Akihiko Nakayama [f]

[a] Civil and Environmental Engineering Department, Universiti Teknologi PETRONAS, Bandar Seri Iskandar, Perak, 32610, Malaysia
[b] Department of Civil Engineering, Ahmadu Bello University, Zaria, Kaduna State, 810107, Nigeria
[c] Global Engineering Centre, Subsea Engineering, TechnipFMC, 600032, India, Chennai
[d] Department of Engineering, Lancaster University, Lancaster, LA1 4YR, UK
[e] Standards Organisation of Nigeria (SON), 52 Lome Crescent, Wuse Zone 7, Abuja, 900287, Nigeria
[f] Department of Environmental Engineering, Universiti Tunku Abdul Rahman (UTAR), 31900, Kampar, Perak, Malaysia

ARTICLE INFO

Keywords:
Optimization
Mooring line design parameters
FPSO RegPSO OrcaFlex, SAFOP

ABSTRACT

Optimization of mooring line design parameters including line azimuth angles, line diameter, line length and mooring radius is presented for a turret-moored FPSO. The optimization procedure is implemented using a Mooring Optimization Tool for FPSO (MooOpT4FPSO), which is an in-house optimization tool purposely developed for this purpose. The tool is a synchronisation of the Regrouping Particle Swarm Optimization (RegPSO) algorithm with commercial software, OrcaFlex. Case studies using a validated numerical FPSO model moored with multicomponent mooring lines acted upon by non-collinear wave, wind and current were analysed using the developed tool. To take into consideration the interaction of the riser system in the optimization procedure, the integrated design methodology was adopted where the riser safe operation (SAFOP) zone diagram combined with the offset diagram is used for the verification/assessment of the design criteria of the risers and mooring lines. The optimized FPSO model offsets in eight directions are found to be within the riser safe operation zone. Based on the results, the tool was able to simultaneously optimise the mooring line diameter, line length, mooring radius, and azimuth angles of the turret FPSO to achieve a specific offset. Application of the tool can help the industry save material (by reduction of line diameter and length) and consequently the overall project cost, in addition to the reduction of structural payload exerted on the platform. Furthermore, the tool has an automatic search capability, which is an improvement to the conventional mooring design approach that is based on a trial-and-error approach.

1. Introduction

Mooring system design entails consideration of several factors including the composition of the mooring lines, type of platform to be moored, environmental conditions and the time the platform will remain anchored in position. Dynamic positioning systems, tethers, mooring lines, or a combination of both are used to maintain floating platforms in position. As a result, the mooring system's ability to maintain the platform in place has a significant influence on the integrity of the risers and the floating platform in general. Hence, the efficiency of the mooring system is largely dictated by the mooring line design parameters, including mooring line material, line length, azimuth angles, diameter, line pretension, mooring radius etc. However, the selection of these design parameters in the currently available procedure is based on a trial-and-error/manual approach which depends mainly on the experience of the engineer, thereby making it extremely time-consuming(Ja'e et al., 2022; da Fonseca Monteiro et al., 2021; Montasir et al., 2019). In addition, the moorings and risers are designed separately with little interaction between the two design teams and mostly using uncoupled analysis(da Fonseca Monteiro et al., 2021; Senra

* Corresponding author.
E-mail addresses: idris_18001528@utp.edu.my (I.A. Ja'e), montasir.ahmedali@utp.edu.my (M.O. Ahmed Ali), yendurianurag@gmail.com (A. Yenduri), c.amaechi@lancaster.ac.uk (C.V. Amaechi), zafarullah@utar.edu.my (Z. Nizamani), akihiko@utar.edu.my (A. Nakayama).

https://doi.org/10.1016/j.oceaneng.2022.112499
Received 11 April 2022; Received in revised form 24 August 2022; Accepted 3 September 2022
Available online 15 September 2022

et al., 2002). The selection of maximum platform offset in both intact and damaged conditions is also done arbitrarily irrespective of the direction. The risers are subsequently designed to satisfy their functional requirement by considering the same offset. This indicates the target offset values as the only connection that links the mooring and riser designs(Ja'e et al., 2022).

Hence, the increased application of FPSOs in deeper waters necessitates the need for an optimum mooring design that ensures minimum platform horizontal excursion during operation(Mehdi and Rezvani, 2007). This is important because substantial platform excursions place an enormous constraint on the workability of offshore floating structures. Thus, an optimum mooring system can be achieved by automating the search component of the mooring design variable in the design procedure to minimise time and effort by eliminating the rigorous trial and error approach, and by considering the mooring design variables as optimization variables.

To actualise this, several studies on the optimization of mooring line design parameters utilising different optimization techniques have been conducted to address the optimization of the mooring system. Maffra et al. (2003), were the first to apply the Genetic Algorithm (GA) in mooring system optimization, with the primary objective of minimising offset of a spread moored vessel through the optimization of the mooring line radius. A mooring pattern optimization of a vessel with a multi-point mooring system was presented in (Alonso et al., 2005) using the Steady-State Genetic Algorithm (SSGA). Also, Mehdi and Rezvani (2007) proposed another mooring optimization procedure using a different variant of GA called Constrained Genetic Algorithm (CGA), the primary objective was to minimise platform offset in surge and sway directions by optimising azimuth angle, mooring radius and the line length. Unlike the preceding procedure, Liang et al. (2019) proposed a multi-objective procedure utilising the Non-dominated Sorting Genetic Algorithm II (NSGA-II) to optimise several mooring design variables in addition to the platform offset and having the capability of providing multiple optimal mooring design.

The application of the Particle Swarm Optimization (PSO) technique was first used for mooring line optimization by (da Fonseca Monteiro et al., 2010) with the objective function of minimising platform offset by considering mooring radius and line azimuth angles as the optimization parameters. An appreciable reduction in platform offset was recorded in the range of 30% and 60% for the two models considered in the work. Furthermore, Monteiro et al. (Da Fonseca Monteiro et al., 2013) assess the implementation of an improved PSO (POSI) technique using line mooring radius, azimuth angle, pretension and line material as optimization variables. The PSOI, when compared with the standard PSO is reported to have an improved convergence rate which is achieved by the application of a velocity update component. The integrated mooring-riser design methodology was also adopted where the riser safe operation (SAFOP) zone diagrams in combination with the mooring line offset diagrams were used to account for the integrity of the risers. The application of a variant of the PSO algorithm associated with an ε-constrained was also applied (Monteiro et al., 2021) for the optimization of deep-water semisubmersible platform using mooring radius, line length and pretension as optimization variables. However, this procedure is an improvement of the one presented in (Da Fonseca Monteiro et al., 2013) with the introduction of a constrained function to efficiently handle constraints and enhance the evaluation of candidate solutions by adopting full non-linear time-domain FE simulations with a coupled model. A more complex approach considering asymmetric mooring configurations was considered in (Monteiro et al., 2016) taking each of the line azimuth angles and mooring radius as optimization variables. The study compares the performance of differential evolution and PSO based on their convergence capability. This was implemented as a spread mooring system of a deep-water semi-submersible platform. In recent times, Montasir et al. (2019), proposed a standalone mooring optimization tool based on quasi-static analysis. The line azimuth angle was used as an optimization variable and successfully implemented using PSO. The proposed tool has optimized offset of a truss spar offset by up to 72% when compared with the original model. However, most of the procedures presented utilised either static or dynamic in the analysis of mooring lines.

Over the years, the interaction between mooring lines and risers has been recognised as an important design consideration, particularly in deep-water operations (Monteiro et al., 2021; Analysis of Stationkeeping Systems for, 2005; Girón et al., 2014; Seymour et al., 2003; Offshore Standard, 2010). As a result, an integrated design methodology has been demonstrated as a better alternative, where the risers, moorings, and floaters are all analysed simultaneously to create a SAFOP and offset diagrams for the riser and moorings respectively. The inclusion of risers in the analysis of floating platforms has been reported as having a significant influence on their natural periods, damping, as well as slow drift responses (Chakrabarti et al., 1996). In another study (Garrett et al., 2003), the inclusion of risers in the analysis was found to have considerable contributions to surge/sway coupling, and as a result the low-frequency motion response. For this reason, the integrated riser-mooring design methodology was regarded as potentially beneficial in deep water platform operations, particularly in terms of the overall system safety, response, and cost(Girón et al., 2014). By incorporating all the components in a single model throughout the study, the technique enables for efficient incorporation of the interaction between the riser, mooring, and platform (Monteiro et al., 2016; Garrett et al., 2003). Furthermore, previous studies have demonstrated the inclination of the oil and gas industries toward full integration of the mooring and riser design procedure(Senra et al., 2002; Correa et al., 2002).

Thus, this paper presents an optimization procedure of mooring line design parameters using the Mooring Optimization Tool for FPSO (MooOpT4FPSO). The tool is an in-house optimization tool, which is an integration of the Regrouping Particle Swarm Optimization (RegPSO) algorithm and OrcaFlex. The tool has the capability of optimising mooring line parameters of turret FPSO supported with 12 or 9 mooring lines. In addition, the tool is configured to take into consideration of the mooring line parameters, it is not limited by the position of the turret or the type of mooring line system (catenary or taut), thus can be utilised for both internal and external turret. Utilising the tool, mooring line design parameters; mooring line diameter, line length (middle segment), mooring radius, and azimuth angles of a turret FPSO were simultaneously optimized. The integrated mooring-riser methodology was incorporated to consider the interaction of the riser in the procedure. The paper considered twelve mooring lines azimuth angles, line diameter, mooring radius, and line length as optimization variables. The superimposition of the riser safe operation (SAFOP) zone and the offset diagram reveals the optimized mooring parameters as sufficient in maintaining platform offset within the SAFOP Apart from successfully having the capability of optimising the platform offset, the tool has the flexibility of utilising the robust capability of the OrcaFlex software utilising both static and dynamic analysis.

1.1. Selection of optimization variables

The mooring system considered in this study is an internal turret consisting of taut and catenary mooring lines. This version of MooOpT4FPSO has the capability of optimising mooring line parameters of turret FPSO with 12 and 9 lines, i.e., 4 × 3 and 3 × 3 mooring configuration respectively as illustrated in Fig. 1(a and b). Each of the lines comprises a chain-polyester -chain segment distributed equally and at the same pretension characteristic value of 1420 kN. The mid-section of each of the mooring lines is of the same length and diameter. Thus, the mooring line design variable of each line identified to influence the performance of the mooring system was adopted as the optimization variable. For each of the mooring configurations, the azimuth angles of the central lines of each group, i.e., lines #1,2,3,4 for 4 × 3 or lines #1,2,3 for 3 × 3, are considered optimization parameters. Thus, MooOpT4FPSO considers a total of 7 or 6 mooring line parameters as

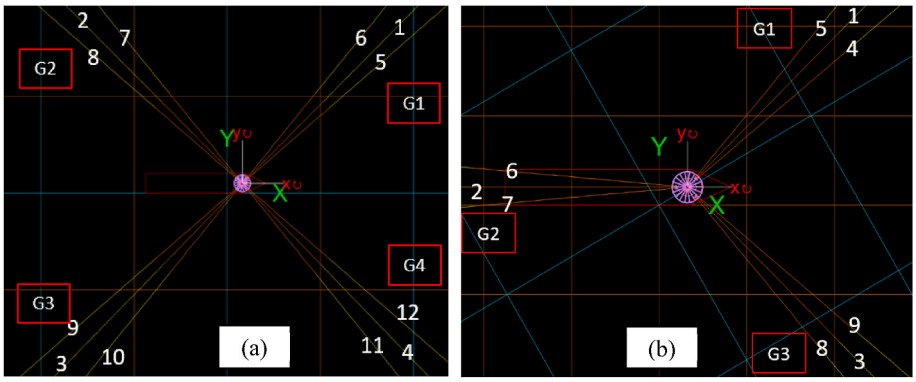

Fig. 1. Layout of turret mooring configuration: (a) 4 x 3 configuration (b) 3 x 3 configuration.

optimization parameters, i.e., 4 or 3 azimuth angles, in addition to mooring radius, mooring line length (of mid-segment) and line diameter. The case is automatically selected depending on the number of mooring lines defined by the user.

1.2. Objective function

The problem presented here is a typical constrained optimization problem, expressed mathematically in Equation (1). The aim is to minimise the objective function f(x) which in this case is the FPSO surge offset. Thus, the primary objective of the optimization procedure is to optimise line parameters that will minimise surge offset of turret FPSO, which has been identified as the most sensitive response.

$$minimize\, f(offset) \tag{1}$$

$$subject\ to\ g_i(offset) \leq threshold\ of\ success,\ i, \ldots, m$$

Where the *threshold of success* is the maximum allowable platform offset defined for the problem, while $g_i(offset)$, is the global best platform offset for each iteration.

The integrated riser-mooring design methodology elaborated in(Ja'e et al., 2022; Girón et al., 2014) and adopted in (da Fonseca Monteiro et al., 2021) has been incorporated herein. Adopting this approach as a component of the optimization procedure is considered more realistic in terms of ensuring the interaction of risers is taken into consideration. This methodology ensures the platform excursion/offset is maintained within the riser safe operation zone (SAFOP).

Thus, the objective of the integrated riser-mooring design methodology is expressed in Equation (2)

$$f = \frac{\sum_{i=1}^{ndir} SAFOP\ (i) - platform\ offset\ (i)}{ndir} \tag{2}$$

where, i is the number of directions considered ($i = 1, ndir$), which should be at least 8, *SAFOP* (i) is the riser safe operation zone in each direction, i recorded in meters, while *platform offset* (i) is the platform excursion obtained using the mooring system, and in the same directions.

1.3. Constraints

The maximum allowable mooring tensions are based on the guidance provided in section 7.2 of the API-RP-2SK (Design and Analysis of Stationkeeping, 2005) specifying 60% and 80% of the minimum breaking load (MBL) when considering dynamic analysis in intact and damage conditions respectively. Thus, the tension constraints are expressed in Equation (3).

$$CTsn_{max} = \begin{cases} \dfrac{Tsn_{max}}{MBL} - 0.6 \\ 0,\ Otherwise \end{cases},\ if\ \frac{Tsn_{max}}{MBL} \geq 0.6 \tag{3}$$

Where, Tsn_{max} is the maximum mooring tension in all lines of a given candidate solution.

2. The optimization tool

2.1. Mooring Optimization Tool for FPSO

The in-house optimization tool named Mooring Optimization Tool for FPSO (MooOpT4FPSO) is a numerical optimization tool developed to optimise mooring line design parameters of turret moored FPSO. The tool is an integration of a Regrouping Particle Swarm Optimization (RegPSO) algorithm with OrcaFlex. This version of MooOpT4FPSO has the capability of simultaneously optimising azimuth angles, mooring line lengths, line diameter and mooring radius of an FPSO turret mooring system consisting of 9 and 12 mooring lines.

MooOpT4FPSO communicate with OrcaFlex in the MATLAB environment through the dynamic link library. Implementation of the optimization procedure includes a complete definition of the FPSO model including the mooring system and environmental loading in OrcaFlex. The OrcaFlex data file is then utilised by the RegPSO algorithm in the MATLAB environment to initialise and assign the mooring line parameters to each line in the OrcaFlex model from a user-defined range. The initialisation of the population of candidate solutions is randomly generated and iteratively updated in the process. For each iteration, dynamic analysis is performed, and a set of mooring line parameters is saved. In each case, individual candidate solutions are evaluated to assess their fitness by the objective function which in turn guides the search process to an optimum solution(Ja'e et al., 2022). This procedure is repeated based on the defined number of particles and iterations until an optimized solution is obtained. An optimized solution here refers to mooring line parameters that yield the minimum platform offset. Fig. 2 illustrates the data flow diagram of the optimization tool.

The developed optimization tool has an interactive Graphical User Interphase which as illustrated in Fig. 3 has 5 major components, namely: (1) the OrcaFlex Path; where the user specifies the path of OrcaFlex on the computer (2) User-defined input; this is where the user defines the optimization and line parameters. (3) The Run, Plot, and Log tabs. (4) Outcomes of optimization; here the optimized mooring line parameters are displayed, and (5) the plot area; the plan of optimized lines with their azimuth angles are displayed.

Firstly, implementation of the optimization procedure requires the user to define the OrcaFlex path on the computer. Secondly, the mooring design parameters and optimization settings are defined. Using the run tab, the optimization process is started. Upon completion of the optimization process, the plot is generated using the plot tab. To view the

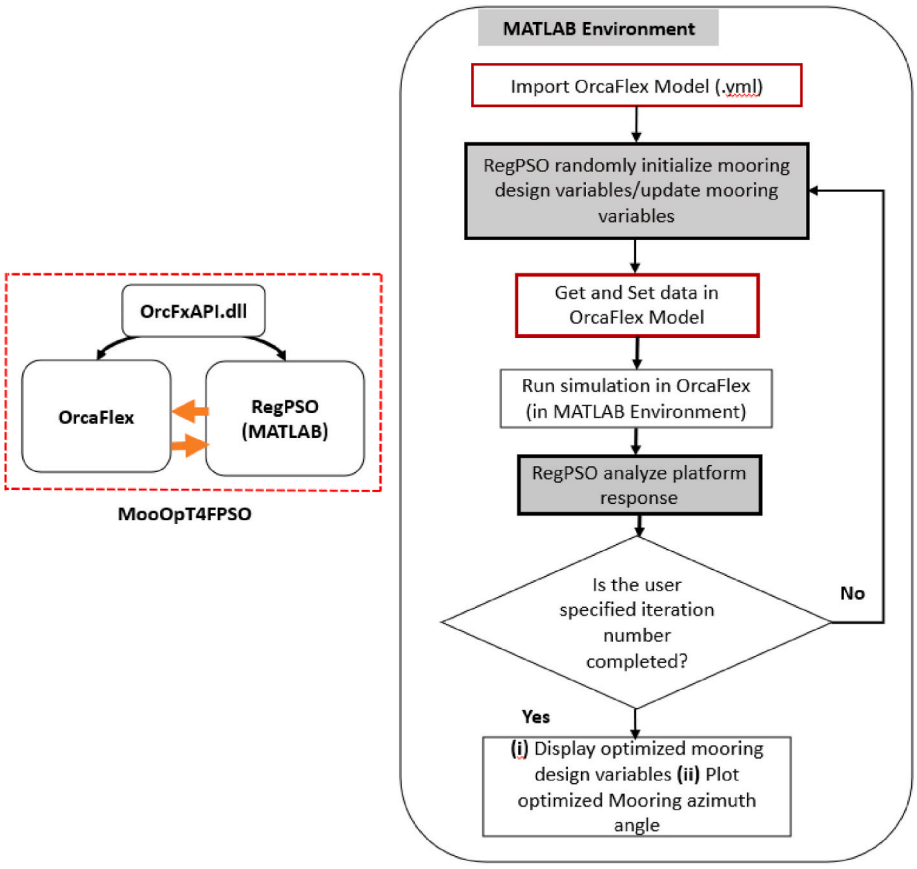

Fig. 2. Data flow working diagram of the optimization tool **(MooOpt4FPSO)**.

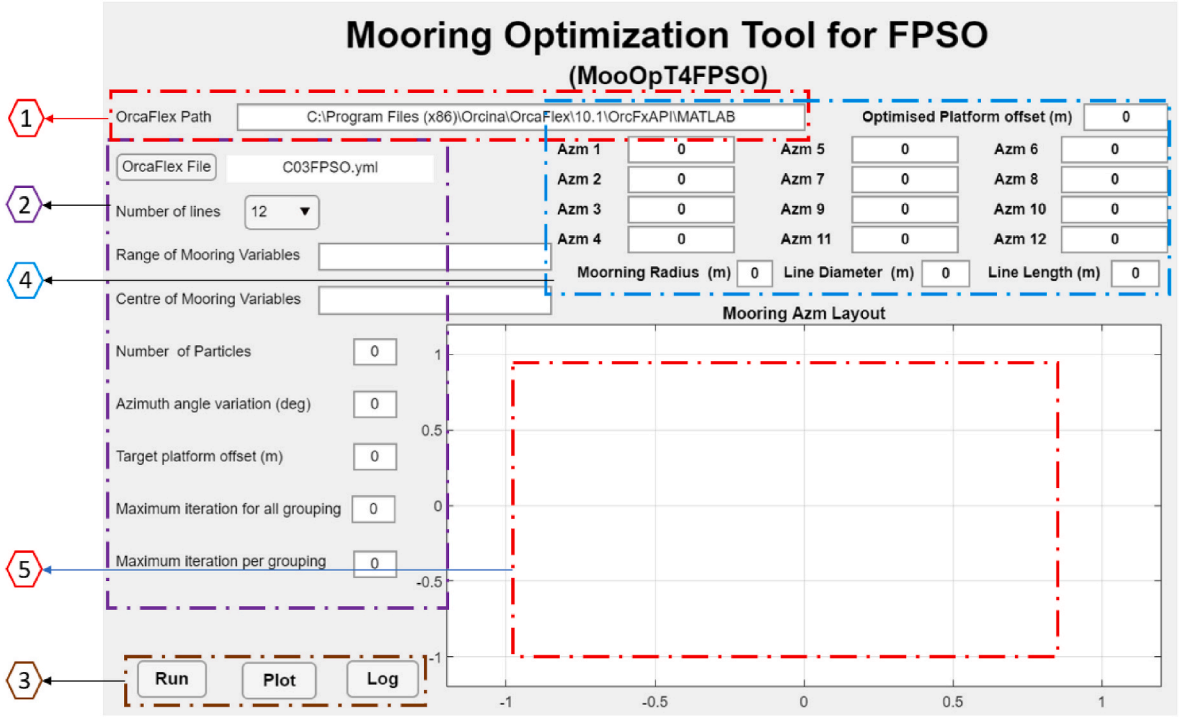

Fig. 3. Graphical User Interface of MooOpT4FPSO illustrating the major component.

detail of optimization settings or error reports the Log tab is used.

2.2. Regrouping Particle Swarm Optimization

The Regrouping Particle Swarm Optimization (RegPSO) technique is a variant of the PSO developed to address the problem of premature convergence identified as a shortcoming of the standard PSO algorithm (Evers and Ghalia, 2009). The algorithm has the computational capability to identify when premature convergence (viz, stagnation) occurs and regroup the particle into a new search space large enough to allow for an efficient search to enable them to escape stagnation and allow the entire swarm to continue making progress rather than restarting as proposed in other studies (Kaucic, 2013).

It is important to note that the standard PSO is effective before being prematurely converged. Thus, the RegPSO algorithm still utilizes the original position and velocity update equations. Hence the main improvement is to liberate the swarm from premature convergence via an automatic regrouping mechanism. Fig. 4 illustrates the flow chart of the RegPSO algorithm.

All particles are randomly picked from all the problem dimensions toward the global best by using the update Equations in 4 and 5.

$$\vec{x_i}(k+1) = \vec{x_i}(k) + \vec{v_i}(k+1) \tag{4}$$

$$\vec{v_i}(k+1) = w\vec{x_i}(k) + c_1\vec{r_1}(k) \circ (\vec{p_i}(k) - \vec{x_i}(k)) + c_2\vec{r_2}(k) \circ (\vec{g_i}(k) - \vec{x_i}(k)) \tag{5}$$

Where k is the current iteration, $\vec{v_i}$ is the velocity vector, $\vec{x_i}$ is the position vector of particle i while w is the static inertia weight. c_1 and c_2 stand for cognitive and social acceleration coefficients respectively, $\vec{p_i}$ is the personal best of particle i and $\vec{g_i}$ the global best of the swarm. The $\vec{r_1}$ and $\vec{r_2}$ are n-dimensional column vectors consisting of pseudo-random numbers selected from a uniform distribution.

2.2.1. Detection of premature convergence

Depending on the number of particles defined in the process, some particles may fail to find a better solution (i.e., a new global best) over a long simulation time, in which case, the particle will tend to continue to move closer to the unchanged global best until all other particles eventually prematurely converged (occupy the same location in space), thereby approximating a local solution rather than a global one. Consequently, progress toward the global best will cease and the process will instead continue to refine the local minimizer with no room for further improvement.

For this reason, the RegPSO determine the distance between the particles as a measure of how close they are to each other to monitor when they eventually converged to the same region or stagnate. This

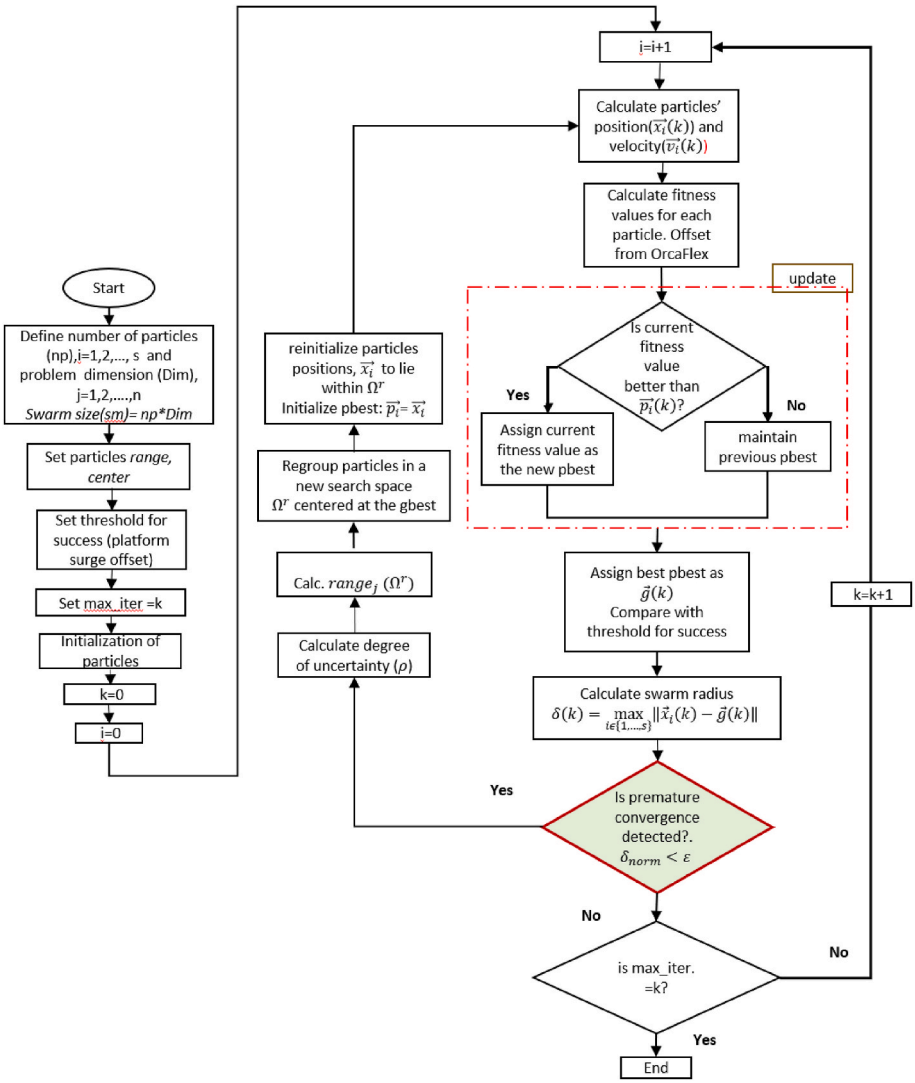

Fig. 4. Flow chart of RegPSO algorithm.

occurrence (premature convergence) is detected from the measurement of maximum swarm radius between particles using Equation (6), initially introduced by Van den Bargh (Van Den Bergh, 2007). For each iteration, the swarm radius $\delta(k)$ is calculated in the n-dimensional space of any particle from the global best.

$$\delta(k) = \max_{ie\{1,\ldots,s\}} \vec{x}_i(k) - \vec{g}(k) \tag{6}$$

If Ω is considered as the search space and the range of particle dimensions represented by the vector, $\overrightarrow{range}(\Omega)$. Then, the diameter of the search space is taken as $dia(\Omega) = range\ \Omega$. The particles are considered too close to each other when the normalized swarm radius (δ_{norm}) is less than the stagnation threshold (ε) as depicted in Equation (7).

$$\delta_{norm} = \frac{\delta(k)}{dia(\Omega)} < \varepsilon\ ,\ where\ \varepsilon = 1.1\ x10^{-4} \tag{7}$$

2.2.2. Regrouping of swarm

Once the condition in Equation (7) is met (i.e., premature convergence detected), the swarm is automatically regrouped into a new search space centred on the global best, using the regrouping factor shown in Equation (8).

$$\rho = \frac{6}{5\varepsilon} \tag{8}$$

The range of each problem dimension defining the new search space, Ω^r are determined by either the magnitude of the regrouping factor, ρ, or the degree of uncertainty inferred on each dimension from the maximum deviation from the global best.

It is important to state here that the degree of uncertainty on each of the dimensions overall particles is computed using Equation (6) while Equation (9) is used to compute the maximum deviation of any one particle.

$$range_j(\Omega^r) = \min\left(range_j(\Omega^r),\ \rho \max_{ie\{1,\ldots,s\}} \left|x_{i,j}(k) - g_j(k)\right|\right) \tag{9}$$

In each case, each particle is randomly regrouped about the global best within the new search space (Ω^r) according to equation (7), this process makes the randomized particle remain within the Ω^r with respect to the defined lower and upper bounds defined in Equations (12) and (13).

$$\vec{x_i}(k+1) = \vec{g_i}(k) + \vec{r_i} \cdot \overrightarrow{range}(\Omega^r) - \frac{1}{2} \cdot \overrightarrow{range}(\Omega^r) \tag{10}$$

Where, $\vec{r_i}$ is a vector of the problem dimension

$$[r_1,\ r_2,\ \ldots,\ r_n,\ ] \tag{11}$$

$$x_j^{L,r} = g_j - \frac{1}{2}\ range_j(\Omega^r) \tag{12}$$

$$x_j^{U,r} = g_j + \frac{1}{2}\ range_j(\Omega^r) \tag{13}$$

L and U in Equations (9) and (10) represent lower and upper limits respectively.

Once the regrouping of the particle is implemented as highlighted in the preceding section, the standard PSO continues as usual. This procedure is repeated iteratively.

2.3. OrcaFlex

OrcaFlex is a 3D non-linear finite element software used for the design and analysis of offshore oil and gas structures and Marine systems such as mooring systems, risers, and marine renewables. It has the capabilities of performing Static and dynamic analysis, fatigue analysis and modal analysis, etc. It also has the capability of implementing both quasi-dynamic and fully coupled analysis.

3. Description of model

3.1. The FPSO model

In implementing the optimization procedure, a validated turret moored FPSO model was used as in(Kim et al., 2005). The model consists of 12 multi-component mooring lines configured into 4 groups, each group consisting of 3 lines, in addition to 13 steel catenary risers as shown in Fig. 5. The FPSO, mooring line and riser system design parameters are depicted in Tables 1 and 2.

3.2. Environmental data and prediction of wind and current forces

The study was conducted using a water depth of 1829m considering 100-year hurricane conditions of the Gulf of Mexico. The JONSWAP wave spectrum having a significant wave height of 12.19m and a peak period of 14 s acting at 180° was used as illustrated in Fig. 6. The wind loading was generated using the Norwegian Petroleum Directorate (NPD) spectrum at 150° with a mean velocity of 41.12 m/s acting at 10m height. In addition, a current profile with a varying velocity of 0.941 m/s to 0.0941 m/s from mean sea level to the sea bed is used[24].

3.3. Functionality of RegPSO

To determine the functionality of the RegPSO component of the tool, the RegPSO algorithm is validated using seven mathematical benchmark functions, including Ackley, the Griewangk, Quadric, Quartic Noise, Rastrigin, Rosenbrock, and weighted sphere as detailed in Table 3. These benchmarks were tested based on a varying number of particles and iterations. In each case, the problem dimension was maintained as 10, with a maximum of 30 particles at 250 iterations. The percentage of range to which each dimension is to be clamped (i.e., velocity clamping) is maintained at 15% as recommended by Liu et al., 2005[25] because it performs better than the traditional 50%.

These functions are selected to test the computational capability of the RegPSO algorithm to optimise both uni-modal and multimodal functions. For example, Ackley, Rastrigin, and Rosenbrock's functions are multi-modal while weighted sphere and the Griewangks functions are unimodal. In each case, the existence of local minima tends to increase with increasing problem dimensionality. In this case, considering the mooring line design variables are less than 10, so we maintain a maximum dimension of 10 to test the capability by varying the number of particles and iterations. For each function, two trial was conducted to

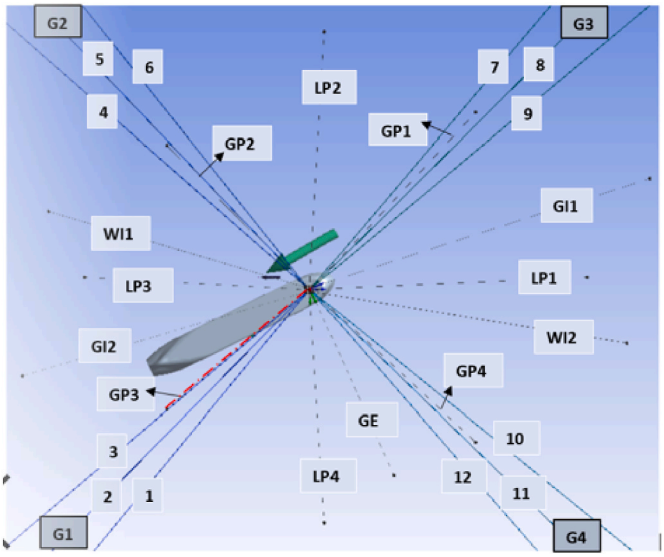

Fig. 5. Layout of Mooring-riser systems of turret FPSO.

Table 1
FPSO main design parameter (Kim et al., 2005).

Parameter	Symbol	Unit	Quantities
Vessel size		kDWT	200
Length between perpendicular	L_{pp}	m	310
Breadth	B	m	47.17
Height	H	m	28.04
Draft (80% loaded)	T	M	15.121
Displacement	V	MT	186051
Block coefficient	C_b		0.85
Surge centre of gravity from turret	CGx	m	−109.67
Heave centre of gravity from mwl	CGy	M	−1.8
Frontal wind area	A_F	m^2	4209.6
Transverse wind area	A_T	m^2	16018.6
Roll radius of gyration at CG of turret	R_{xx}	M	14.036
Pitch radius of gyration at CG of turret	R_{yy}	M	77.47
Yaw radius of gyration at CG of turret	R_{zz}	M	79.3
Turret in centre line behind F_{pp}	Xtur	M	38.75
Turret diameter	Dtur	M	15.85
Turret elevation below tanker base		M	1.52

Table 2
Mooring line Details (Kim et al., 2005).

Legend	Top Segment	Middle Segment	Lower Segment
Type	Chain	Polyester	Chain
Diameter(mm)	95.3	160	95.3
Length (m)	91.4	2438	91.4
Wet weight (kg/m)	164.63	4.5	164.63
Effective Modulus (kN)	820900	168120	820900
Breaking Load (kN)	7553	7429	7553
Normal drag coefficient, C_{DN}	2.45	1.2	2.45
Normal added inertia coefficient, C_{IN}	2.0	1.15	2.0

Table 3a
Particulars of steel catenary risers.

	LP	GP	WI	GI	GE
Top tension (kN) rowhead	1112.5	609.7	2020.0	1352.8	453.9
Outer diameter(mm) rowhead	444.5	386.1	530.9	287.0	342.9
EA (kN) rowhead	18.3 x106	10.3 x106	18.6 x106	31.4 x106	8.6 x106
Wet Weight (N/m) rowhead	1037	526	1898	1168	423

allow for average comparison.

3.4. Implementation of the optimization procedure

The tool utilizes an updated OrcaFlex data file linked with the RegPSO code to automatically search and update mooring design variables taking advantage of the robust functionality of the software. The functionality of the tool is influenced by many parameters, including the number of particles, dimension of the problem, number of iterations and other parameters as listed in Table 4. The number of particles particularly dictates the size of the swarm (i.e., swarm = no of particle * dimension). However, although the larger the number of particles the greater the chances of finding a global minimum, this can also result in parallel random search and in that case increasing the computational time. A varying number of particles ranging from 10 to 50 have been reported as appropriate for different variants of PSO (Piotrowski et al., 2020). On the other hand, the number of iterations together with the specified success threshold dictate the stopping criteria.

For each mooring variable, a range and central (median) value is defined to guide the search of the protocol to the global best.

Table 3b
Benchmark functions.

Benchmarks	Function	Initial range of x_j
Ackley	$f(\vec{x}) = 20 + e - 20e^{-0.2\sqrt{\frac{\sum_{j=1}^{n} x_j^2}{n}}} - e^{\frac{\sum_{j=1}^{n}\cos(2x_j\pi))}{n}}$	$-32 \le x_j \le 32$
Griewangk	$f(\vec{x}) = 1 + \sum_{j=1}^{n}\frac{x_j^2}{4000}\prod_{j=1}^{n} cos\left(\frac{x_j}{\sqrt{j}}\right)$	$-600 \le x_j \le 600$
Quadric	$f(\vec{x}) = \sum_{j=1}^{n}(\sum_{j=1}^{n} j.x_j)^2$	$-100 \le x_j \le 100$
Quartic Noise	$f(\vec{x}) = random(0,1) + \sum_{j=1}^{n} j.x_j^4$	$-1.28 \le x_j \le 1.28$
Rastrigin	$f(\vec{x}) = 10n + \sum_{j=1}^{n}(x_j^2 - 10\cos(2x_j\pi))$	$-5.12 \le x_j \le 5.12$
Rosenbrock	$f(\vec{x}) = \sum_{j=1}^{n-1}(100(x_{j+1} + x_j^2)^2 + (x_j)^2)$	$-30 \le x_j \le 30$
Weighted Sphere	$f(\vec{x}) = \sum_{j=1}^{n} j.x_j^2$	$-5.12 \le x_j \le 5.12$

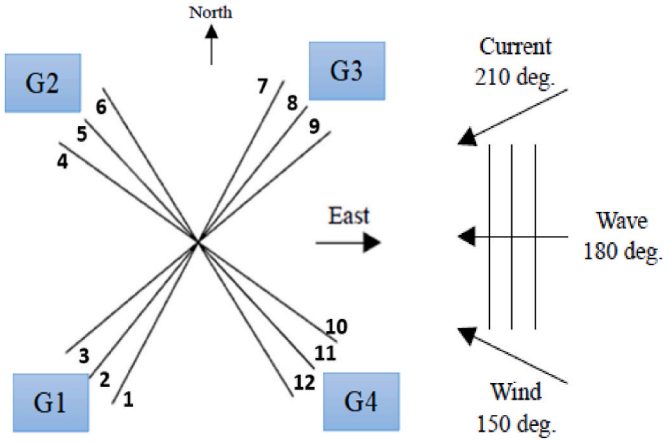

Fig. 6. Illustration of the wave, wind, and current directions.

Table 4
RegPSO parameter setting.

Parameter	Value
Number of particles	Up to 10
Dimension of problem	6 and 7
Stagnation threshold	1.1*10^ (−4)
Regrouping factor	1.2/Stagnation threshold
Inertia weight	[0.9,0.4]
Max velocity clamping %	0.15
No. of iterations per group	Varied
Max iteration overall grouping	Varied

3.5. Integrated design methodology

Previously, some of the few available mooring optimization procedures considered only the mooring lines for the prediction of optimal platform offset without due consideration to the integrity of the risers (Montasir et al., 2019; Senra et al., 2002). In this study, we incorporated the integrated design methodology which is implemented based on the flow chart illustrated in Fig. 7. The procedure of producing SAFOP and offset diagrams.

The SAFOP is a polar diagram defining the horizontal displacement within which the top and the bottom connection point of the risers must remain to ensure none of the risers exceeds any of its design criteria in

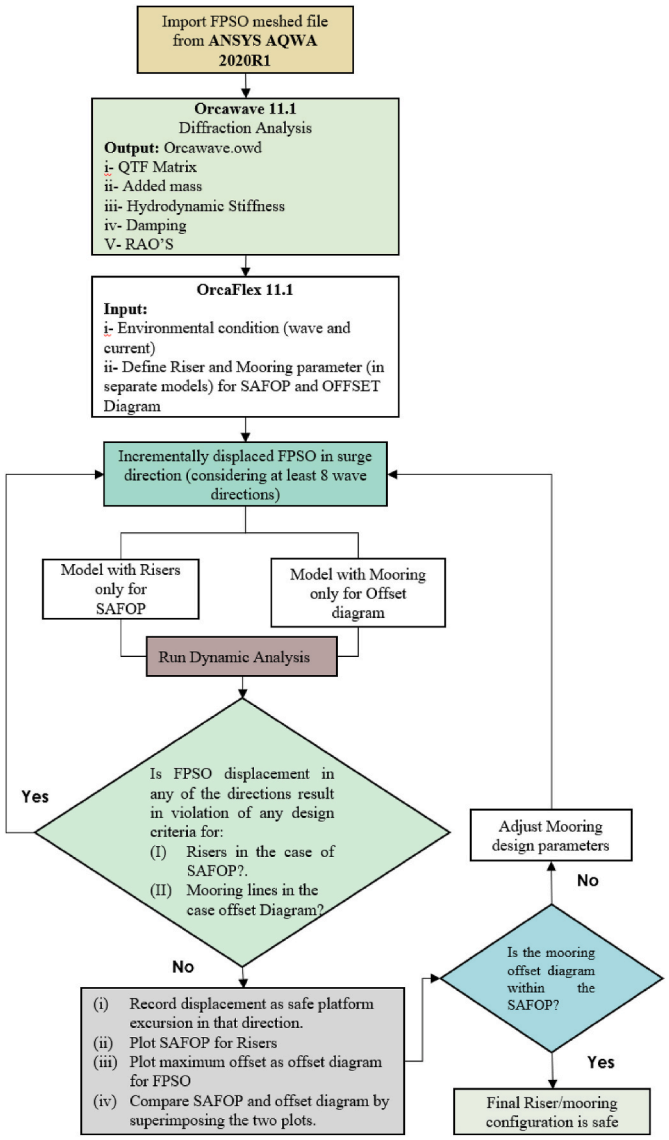

Fig. 7. Flow chart for implementation of Safe Operation Zone (SAFOP) and offset Diagram for the Mooring system.

any of the wave directions considered. Here, we considered the 8 wave directions in producing the diagrams.

The offset diagrams on the hand are also polar diagrams that define the expected maximum horizontal excursions of the floater.

The superposition of the two diagrams gives a visual verification/assessment of the design criteria for the riser and mooring lines.

4. Results and discussions

4.1. Validation of FPSO model for hydrodynamic data

The validation results (AQWA) consisting of static offset, free decay, and hydrodynamic response results in six degrees of freedom (6DOF) degrees well with the published results (Montasir et al., 2019) as shown in Fig. 6, Tables 5 and 6 respectively. Fig. 8 compares the mooring restoring forces from both models, which tend to linearly increase with increasing platform excursion. However, a slight variation of 3% between the WINPOST and AQWA model is observed at about 80m–90m excursions.

From Table 5, the natural periods of the AQWA model for all the degrees of freedom considered are within the range of both published

Table 5
Comparisons of Validation free decay results.

	Periods(sec)			Damping (%)		
	AQWA	WINPOST	OTRC	AQWA	WINPOST	OTRC
Surge	205.2	204.7	206.8	3.7	4.4	3.0
Heave	10.8	10.8	10.7	4.5	11.8	6.7
Roll	12.7	12.7	12.7	3.2	0.7	3.4
Pitch	10.7	10.8	10.5	7.5	10.5	8.0

experimental and simulation results. The same trend is observed in the case of the damping ratios, with the AQWA model having damping ratios closer to the published experimental results. Overall, the results compare well with the published restoring force, natural periods, and damping ratios.

Table 6 statistically compares the responses of the AQWA model in 6DOF with the published results. This reveals close agreement with the published results, thereby proving the accuracy adopted in the validation process.

4.2. The functionality of the RegPSO algorithm

Table 7 shows the statistical performance of RegPSO code in optimising various mathematical benchmark functions with a different number of particles. It can be observed that with an increasing number of particles the global minima also decrease. This is due to the consequent increase in swarm size which increases the number of possible solutions. Thus, this indicates the capability of the RegPSO in finding the optimum solution for the selected mathematical benchmark functions.

For the mean of the two trials conducted for each benchmark, it can be observed that the code has successfully minimised Ackley function by 99%, the Griewangk function by 90%, Quadric by 99.9% and Quartic Noisy by 96.1%. The code also minimises Rastrigin by 82%, Rosenbrock by 98% and weighted sphere by 100%. The Rastrigin benchmark function result is particularly impressive because the benchmark generally returns high function values due to the stagnation of the swarm.

Table 8 shows the statistical comparison of RegPSO performance across seven benchmark functions with an increasing number of iterations. A similar trend was observed in Table 7. The code was able to minimise the Ackley function by 97%, the Griewangk function by 72%, the Quadric function by 99% and Quartic Noisy by 80%. It has also minimised the Rastrigin function by 56%, Rosenbrock function by 58% and weighted sphere by 99%.

Observing Tables 7 and 8, it is clear to notice the drop in values with an increasing number of particles and number of iterations respectively for all the benchmarks. This indicates the capability of the code to minimise the seven mathematical benchmark functions consisting of uni, bi and multi-modal functions by explicitly exploring and exploiting the search space. It is also interesting to observe the consistency of the code across all the benchmarks considered.

4.3. Case studies of optimization problems

To demonstrate the functionality of the Optimization tool (MooOpT4FPSO), two case studies considering the validated model described in section 3 were used to optimise the mooring line parameters of the turret FPSO with 4 × 3 and 3 × 3 configurations with 12 and 9 mooring lines.

4.3.1. Case of turret FPSO with twelve taut mooring lines

Fig. 9 illustrates the optimization results from MooOpT4FPSO for turret FPSO with 12 lines. The GUI illustrate the optimized parameters to maintain a platform of 15m and a mooring azimuth layout.

Furthermore, Tables 9 and 10 illustrate the optimal solutions for the mooring design variables.

Table 9 shows the comparison of original and optimized mooring line

Table 6
Comparison of validation results in 6DOF.

	Source	Surge(m)	Sway(m)	Heave(m)	Roll (deg)	Pitch (deg)	Yaw (deg)
Max	AQWA	4.44	11.2	8.33	8.2	3.37	−15.21
	WINPOST	2.29	13.1	10.9	3.5	4.45	−3.4
	OTRC	6.30	10.9	9.11	9.57	4.2	−8.69
Min	AQWA	−60.22	−20.04	−10.45	−7.26	−4.37	−29.72
	WINPOST	−61.30	−21.4	−11.3	−3.6	−4.99	−24.6
	OTRC	−54.10	−13.6	−9.52	−8.77	−4.07	−23.3
Mean	AQWA	−20.77	−0.48	0.11	0.06	0.17	−18.37
	WINPOST	−22.90	−0.09	0.14	−0.1	0.01	−16
	OTRC	−21.10	−0.64	−0.06	−0.08	0.03	−16.8
SD	AQWA	7.97	4.55	2.92	1.45	1.19	5.03
	WINPOST	9.72	4.57	3.08	0.9	1.31	3.8
	OTRC	8.78	4.05	2.81	2.18	1.26	2.46

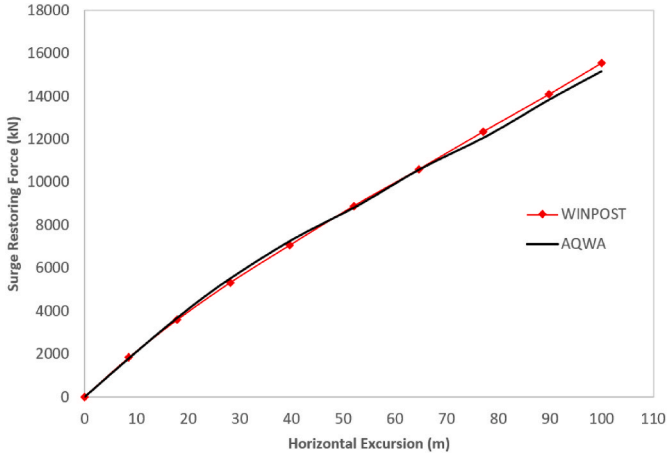

Fig. 8. Comparison of Restoring Behaviour of the WINPOST and AQWA model.

azimuth angles. Other parameters presented are shown in Table 10. Which shows the reduction in line length and diameter and mooring radius, with a consequent reduction in platform offset from 40.8m to 14.99m as specified (target platform offset). This is equivalent to a 63.3% reduction in the platform offset. In addition, the reduction in line length and diameter comes with a reduction in line material and resulting payload. Also, a reduction in mooring radius will yield a consequent reduction in line tension.

4.3.2. *Case of turret FPSO with nine taut mooring lines*

In the case of turret moored FPSO with 9 mooring lines, the 4th row of azimuth angles consisting of lines #4, #11 and #12 as shown in the GUI are not considered as shown in Fig. 10. Tables 11 and 12 compares original and optimized line parameters from MooOpT4FPSO. In each case, the optimized parameters are better than the original in terms of reduction in line length and diameter.

4.3.3. *Case of turret FPSO with twelve catenary mooring lines*

The optimization result for a turret FPSO with 12 catenary mooring lines is illustrated in Fig. 11. The results indicated optimized mooring parameters required to maintain the platform within a 30-m offset as

Table 7
Functionality of RegPSO across Mathematical benchmarks with different numbers of particles.

Benchmark functions	Dimension	No. particle		Number of particles		
				2	10	30
Ackley	10	30	Mean	6.6583	0.16809	0.07034
			Min	4.519	0.11141	0.05609
			Max	8.7979	0.22476	0.08459
			Std	3.0254	0.08015	0.02015
Griewangk	10	30	Mean	1.9885	0.46766	0.19584
			Min	1.5313	0.36529	0.12548
			Max	2.4458	0.57004	0.2662
			Std	0.64665	0.14478	0.0995
Quadric	10	30	Mean	1397.62	4.3421	0.87772
			Min	616.936	1.9549	0.23309
			Max	2178.3	6.7294	1.5223
			Std	1104.05	3.3761	0.91165
Quartic Noisy	10	30	Mean	0.14832	0.01337	0.00578
			Min	0.13059	0.00732	0.0047
			Max	0.16605	0.01942	0.00685
			Std	0.02507	0.00856	0.00152
Rastrigin	10	30	Mean	41.6264	14.8883	7.5733
			Min	38.5929	4.8645	7.1779
			Max	44.6599	24.9121	7.9686
			Std	4.29	14.1758	0.55905
Rosenbrock	10	30	Mean	4344.47	367.807	85.7507
			Min	3761.15	207.586	72.4246
			Max	4927.79	528.027	99.0768
			Std	824.941	226.586	18.8459
weighted Sphere	10	30	Mean	2.8269	0.00045	0.00028
			Min	1.1083	0.00034	0.00028
			Max	4.5455	0.00055	0.00029
			Std	2.4305	0.00015	1.31E-05

Table 8
Functionality of RegPSO across Mathematical benchmarks with different iteration numbers.

Benchmark	Dimension	No. particle		No. of iterations					
				50	100	150	200	250	800
Ackley	10	30	Mean	2.0427	0.69939	0.14082	0.095786	0.07034	4.6915E-7
			Min	1.9482	0.63282	0.11526	0.060066	0.05609	1.606E-7
			Max	2.1371	0.76596	0.16637	0.13151	0.08459	8.7023E-7
			Std	0.13359	0.094147	0.036143	0.050517	0.02015	1.4519E-7
Griewangk	10	30	Mean	0.70807	0.52323	0.32358	0.27586	0.19584	0.0098573
			min	0.62384	0.41003	0.2449	0.18308	0.12548	0.013861
			max	0.7923	0.63643	0.40226	0.36864	0.2662	0. 058867
			std	0.11912	0.16009	0.11127	0.13121	0.0995	0.01552
Quadric	10	30	Mean	118.9254	16.5321	3.9363	1.9285	0.87772	3.1351E-10
			min	54.6702	16.1066	2.9926	0.77378	0.23309	6.0537E-11
			max	183.1805	16.9576	4.8799	3.0832	1.5223	9.5804E-10
			std	90.8706	0.60178	1.3345	1.633	0.91165	2.2243E-10
Quartic Noisy	10	30	Mean	0.029522	0.015955	0.013093	0.007402	0.00578	5.7801E-19
			min	0.028676	0.014012	0.012174	0.006852	0.0047	
			max	0.030367	0.017898	0.014012	0.007952	0.00685	
			std	0.001196	0.002748	0.0013	0.000778	0.00152	
Rastrigin	10	30	Mean	17.0199	8.2907	7.9991	7.9822	7.5733	2.6824E-11
			min	13.2245	8.256	7.9812	7.9753	7.1779	0
			max	20.8152	8.3254	8.017	7.9892	7.9686	1.3337E-9
			std	5.3675	0.049082	0.025337	0.009826	0.55905	1.886E-10
Rosenbrock	10	30	Mean	206.4768	108.6743	88.7519	88.0642	85.7507	0.0039351
			min	190.9286	104.6813	78.4269	77.0515	72.4246	1.7028E-5
			max	222.0251	112.6673	99.0768	99.0768	99.0768	0.018039
			std	21.9886	5.6469	14.6017	15.5742	18.8459	0.0041375
Weighted Sphere	10	30	mean	0.026525	0.004729	0.000626	0.000518	0.00028	9.8177E-14
			min	0.022493	0.00105	0.0006	0.00051	0.00028	1.9112E-14
			max	0.030557	0.008407	0.000655	0.000526	0.00029	2.5244E-13
			std	0.005702	0.005202	4.09E-05	1.13E-05	1.3E-05	5.4364E-14

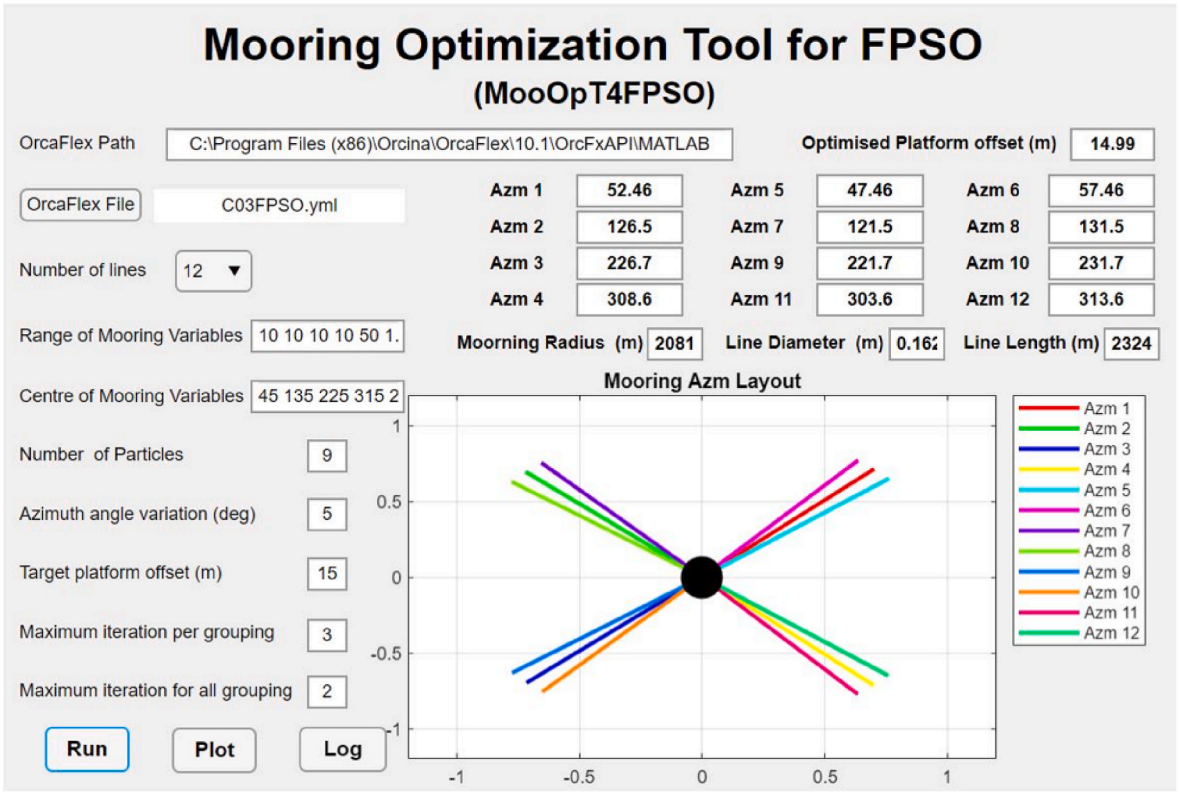

Fig. 9. Complete optimization result for turret FPSO with 12 mooring line.

defined during the analysis. Detailed comparisons are presented in Tables 13 and 14.

Table 13 compares the mooring line azimuth angle of the original and optimized models. On the other hand, Table 14 compares the mooring line length, mooring radius, and line diameter of the original and optimized model. In each case, the optimized parameters present better line parameters, with the 3.4%, 5.2% and 2.8% reduction in mooring line length, diameter, and mooring radius, respectively on

Table 9
Comparison of original and Optimized mooring Azimuth angles.

	Azimuth (°)	
Line	Original	Optimized
Line 1	45	52.46
Line 2	135	126.5
Line 3	225	226.7
Line 4	315	308.6
Line 5	40	47.46
Line 6	50	57.46
Line 7	130	121.5
Line 8	140	131.5
Line 9	220	221.7
Line10	230	231.7
Line11	310	303.6
Line12	320	313.6

Table 10
Comparison of original and Optimized Mooring length, line diameter and Mooring radius.

	Original	Optimized	%Difference
Mooring Length (m)	2438	2324	4.7
Diameter(mm)	170	162	4.7
Mooring Radius(m)	2090	2081	0.43
Surge Offset	40.8	14.99	63.3

every single line. In addition, a significant reduction in platform offset of 67.7% was recorded. The optimized result is consistent with the ones presented for taut moorings thereby confirming the capability of the tool.

4.3.4. Case of turret FPSO with nine catenary mooring lines

Fig. 12 illustrates optimized results of turret FPSO with 9 catenary mooring lines from MooOpT4FPSO.

The detail of the results is further elaborated in Tables 15 and 16. The variations of azimuth angles as illustrated in Table 15 has a direct influence on mooring line length, diameter and the mooring radius as shown in Table 16. Most importantly the resulting optimized line parameters have successfully reduced the platform offset by 64.5%.

This is consistent with the results obtained by other mooring configurations presented using taut moorings.

Table 11
Comparison of original and Optimized mooring Azimuth angles.

	Azimuth (°)	
Line	Original	Optimized
Line 1	50	51.75
Line 2	135	131
Line 3	270	275.1
Line 4	45	46.75
Line 5	55	56.75
Line 6	130	126
Line 7	140	136
Line 8	265	270.1
Line 9	270	280.1

Table 12
Comparison of original and Optimized Mooring length, line diameter and Mooring radius.

	Original	Optimized	%Difference
Mooring Length (m)	2438	2372	3
Diameter(mm)	170	162.1	4.6
Mooring Radius(m)	2090	2088	0.1
Surge Offset	44.2	23.21	47.5

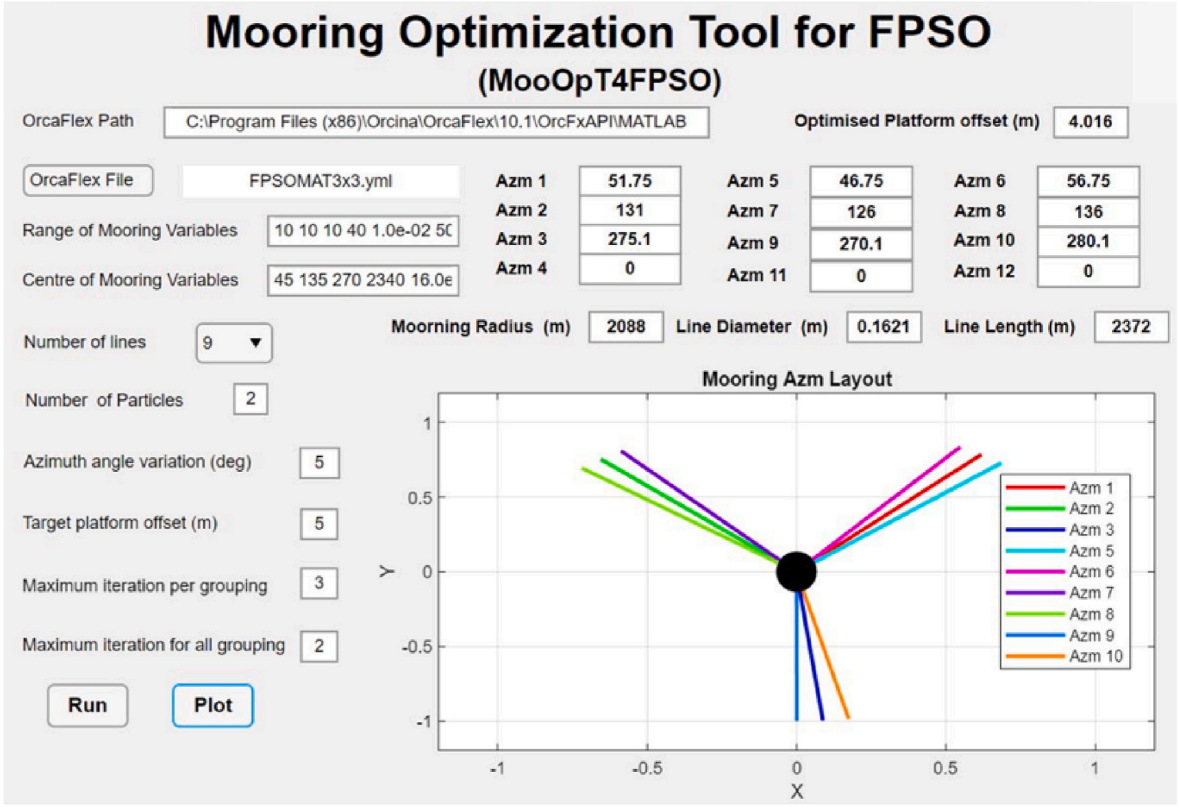

Fig. 10. Complete optimization result for turret FPSO with 9 mooring lines.

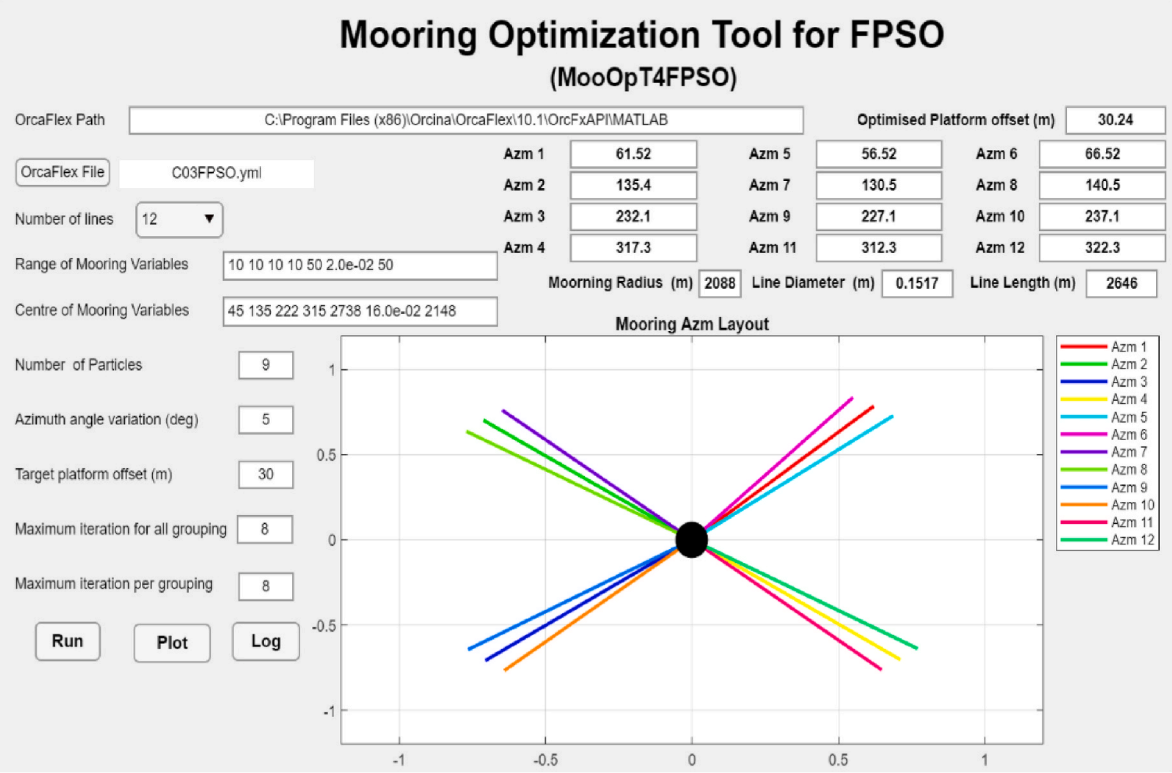

Fig. 11. Complete Optimization result for turret FPSO with 12 Catenary mooring lines.

Table 13
Comparison of original and Optimized mooring Azimuth angles.

	Azimuth (°)	
Line	Original	Optimized
Line 1	45	61.52
Line 2	135	135.4
Line 3	225	232.1
Line 4	315	317.0
Line 5	40	56.53
Line 6	50	66.52
Line 7	130	130.4
Line 8	140	140.4
Line 9	220	227.1
Line10	230	237.1
Line11	310	312.0
Line12	320	322.0

Table 14
Comparison of original and Optimized Mooring length, line diameter and Mooring radius.

	Original	Optimized	%Difference
Mooring Length (m)	2738	2646	3.4
Diameter(mm)	160	151.7	5.2
Mooring Radius(m)	2148	2088	2.8
Surge Offset	93.4	30.2	67.7

4.4. Evaluation of optimized mooring offset with riser SAFOP in intact and damage conditions

4.4.1. Comparison with FPSO with twelve taut mooring lines

The superimposed SAFOP and offset diagram in Fig. 13 compare the maximum offset of the original model with 12 taut lines and optimized mooring configurations (intact and damaged) with the SAFOP limits to ensure the integrity of the risers in all 8 directions considered. From these figures, it can be observed that the optimized mooring configurations maintain the platform within the SAFOP zone of the risers even in the event of a line failure.

4.4.2. Comparison with turret FPSO with nine taut mooring lines

Fig. 14 compares the platform offset of the original FPSO with nine taut moorings, the optimized (intact and damaged) with the SAFOP.

It can be observed for both intact and damaged conditions, the optimized platform offsets in all directions are maintained within the riser SAFOP. While for the original model, platform offset is only maintained in two directions (NE and E).

4.4.3. Comparison with turret FPSO with twelve catenary mooring lines

Fig. 15 illustrate the comparison of platform offset for the original and optimized model from MooOpT4FPSO. This case considers catenary mooring lines in intact and damaged condition.

The optimized platform offset can be observed to be within the SAFOP in all 8 directions while the platform offset from the original model can be seen to go beyond the SAFOP in 4 directions (NW, W, SW, S).

4.4.4. Comparison with turret FPSO with nine catenary mooring lines

In this case, Fig. 16 compare the platform offset of turret FPSO with 9 catenary lines.

Similar to what was observed in Fig. 15, the optimized offset can be observed to be within the SAFOP in all 8 directions compared to the original. Also, in the case of damage, the optimized offset is maintained within the riser SAFOP.

This infers the efficiency of the tool in providing mooring parameters that ensure platform offset is maintained within the risers' safe operation zones.

5. Conclusion

In this paper, we presented an optimization procedure of mooring

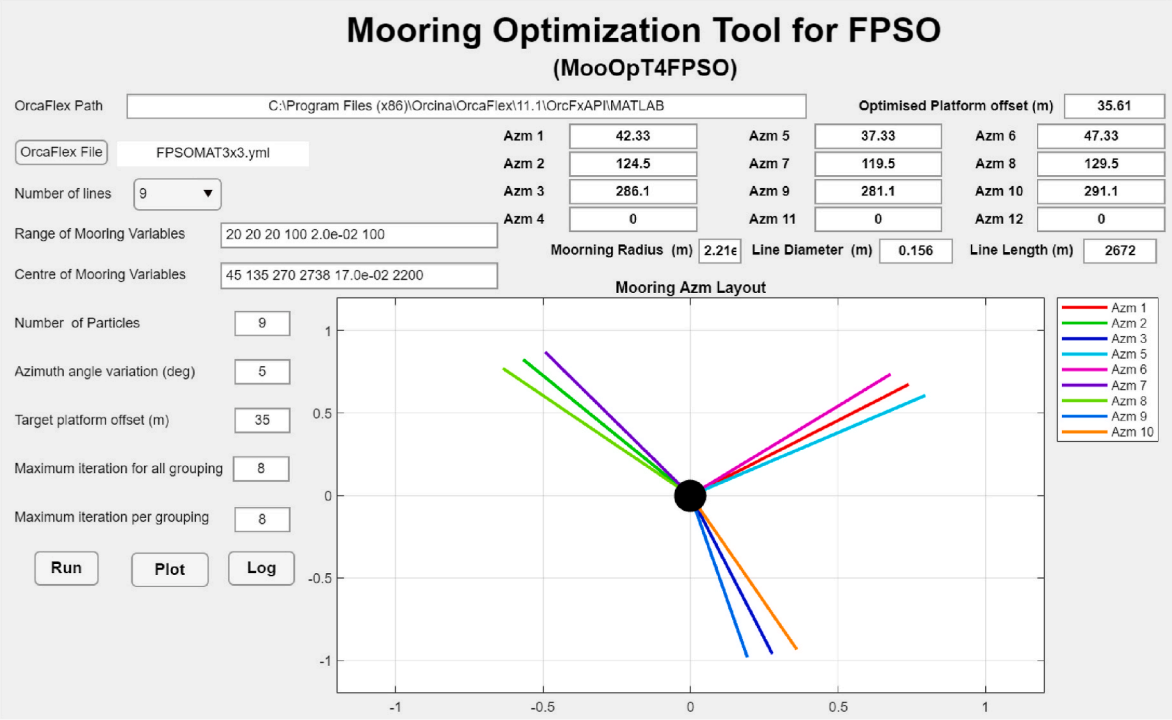

Fig. 12. Complete Optimization result for turret FPSO with 9 Catenary mooring lines.

Table 15
Comparison of original and Optimized mooring Azimuth angles.

	Azimuth (°)	
Line	Original	Optimized
Line 1	50	42.33
Line 2	135	124.45
Line 3	270	286.10
Line 4	45	37.33
Line 5	55	47.33
Line 6	130	119.45
Line 7	140	129.45
Line 8	265	281.1
Line 9	270	291.1

Table 16
Comparison of original and Optimized Mooring length, line diameter and Mooring radius.

	Original	Optimized	%Difference
Mooring Length (m)	2738	2672	2.40
Diameter(mm)	160	156.1	2.40
Mooring Radius(m)	2148	2096	2.42
Surge Offset	100.2	35.6	64.5

line parameters for a turret moored FPSO using a Mooring Optimization Tool for FPSO (MooOpT4FPSO). The tool is an integration of the Regrouping particle swarm optimization (RegPSO) algorithm and a commercial software OrcaFlex. In addition, the integrated riser-mooring design methodology has been incorporated to take into consideration the interaction of the riser, mooring and the FPSO hull. The superimposed riser safe operation zone (SAFOP) and the platform offset diagram are used to assess and ensure that maximum platform offset is maintained within the riser safe operating zone. The specific conclusion from this study are as follows:

1) The Optimization tool has successfully simultaneously optimized mooring line length (mid-segment), line diameter, mooring radius, and azimuth angles of turret FPSO while ensuring platform excursions are maintained within the riser safe operation zone, which is very important.
2) The tool has the computational capability of optimising mooring line parameters of turret FPSO with 12 and 9 mooring lines to achieve target platform offset.
3) From the optimized results, the application of the tool in mooring design can bring a reduction in line material and consequently the overall project cost, in addition to the reduction of payload exerted on the platform.

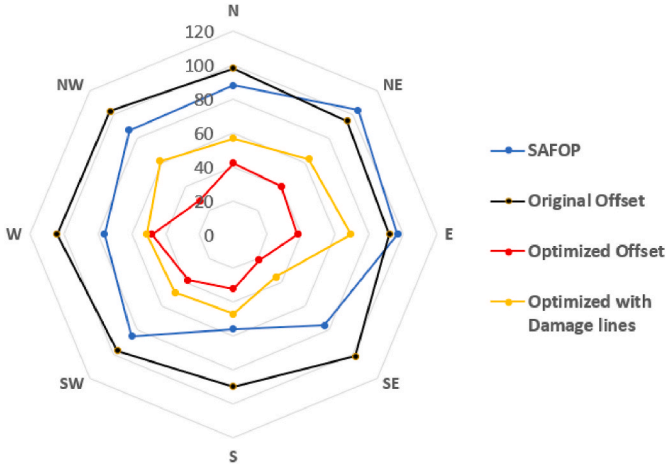

Fig. 13. Comparison of SAFOP and Optimized offset diagrams for FPSO with 12 mooring lines with damaged lines.

CRediT authorship contribution statement

Idris Ahmed Ja'e: Conceptualization, Methodology, Software, Validation, Formal analysis, Writing (original and edit). **Montasir**

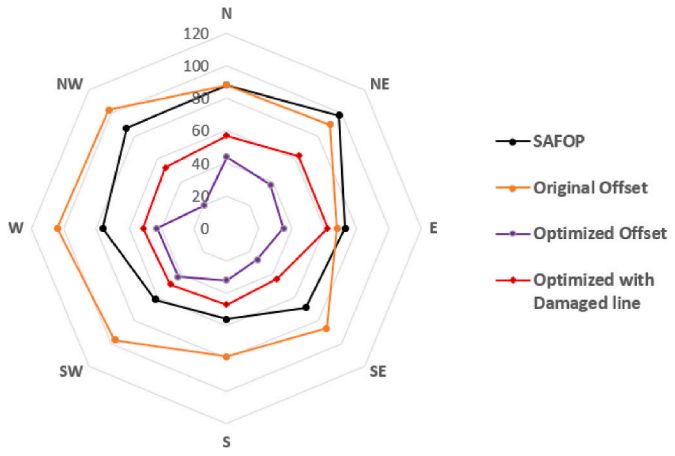

Fig. 14. Comparison of SAFOP and Optimized offset diagrams for FPSO with 9 mooring lines with damaged lines.

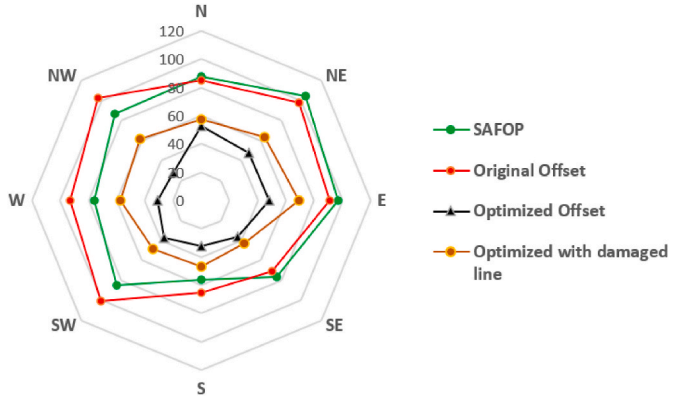

Fig. 15. Comparison of SAFOP and Optimized offset diagrams for FPSO with 12 catenary mooring lines with a damaged line.

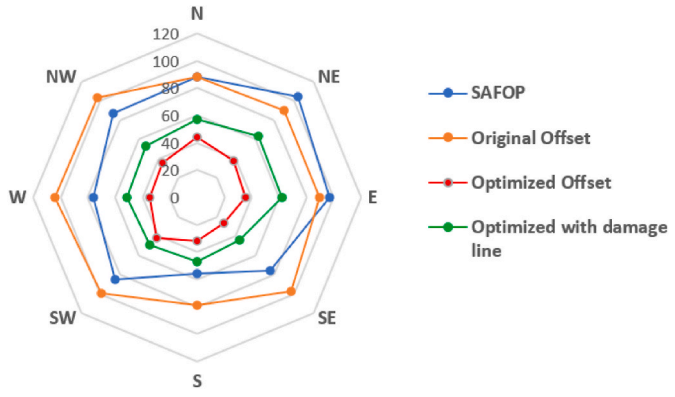

Fig. 16. Comparison of SAFOP and Offset diagrams for FPSO with 9 Catenary mooring lines.

Osman Ahmed Ali: Conceptualization, Methodology, Supervision, Project administration. **Anurag Yenduri:** Methodology, Visualization, Supervision. **Chiemela Victor Amaechi:** Software, Formal analysis, Data curation, Visualization. **Zafarullah Nizamani:** Resources, Visualization, Supervision. **Akihiko Nakayama:** Resources, Visualization.

Declaration of competing interest

The authors declare that they have no known competing financial interests or personal relationships that could have appeared to influence the work reported in this paper.

Data availability

The authors do not have permission to share data.

Acknowledgements

The authors acknowledged the Universiti Teknologi PETRONAS, Malaysia for supporting this research under YUTP 015LC0-116.

References

Alonso, J.J.C., Ivan, F.M.M., Luiz, F.M., 2005. Mooring pattern optimization using genetic algorithms. In: 6th World Congresses of Structural and Multidisciplinary Optimization, Rio de Janeiro, Brazil, pp. 1–9.

Analysis of Stationkeeping Systems for Floating Structures, 2005. A. Design.

Chakrabarti, P., Chandwani, R., Larsen, I., 1996. Analyzing the effect of integrating riser/mooring line design. In: Proceedings of OMAE. American Society of Mechanical Engineers, New York, NY (United States).

Correa, F.c.N., Senra, S.F., Jacob, B.P., Masetti, I.a.Q., Mourelle, M.r.M., 2002. Towards the integration of analysis and design of mooring systems and risers: Part II—studies on a DICAS system. Int. Conf. Offshore Mech. Arctic Eng. 36118, 291–298.

Van Den Bergh, F., 2007. An Analysis of Particle Swarm Optimizers. University of Pretoria.

Design and Analysis of Stationkeeping Systems for Floating Structures, 2005. API, Washington DC.

Evers, George I., Ghalia, M.B., 2009. Regrouping particle swarm optimization:A new global optimization algorithm with improved performance consistency across benchmarks. In: IEEE International Conference on Systems, Man, and Cybernetics, San Antonio, TX, USA, pp. 3901–3908.

da Fonseca Monteiro, B., Albrecht, C.H., Jacob, B.P., 2010. Application of the particle swarm optimization method on the optimization of mooring systems for offshore oil exploitation. In: Proceedings of Second International Conference on Engineering Optimization.

Da Fonseca Monteiro, B., De Lima Jr., M.H.A., Albrecht, C.H., De Souza Leite, B., De Lima, P., Jacob, B.P., 2013. Mooring Optimization of Offshore Floating Systems Using an Improved Particle Swarm Optimization Method, vol. 1. https://doi.org/10.1115/OMAE2013-11096 [Online]. Available:

da Fonseca Monteiro, B., Baioco, J.S., Albrecht, C.H., de Lima, B.S.L.P., Jacob, B.P., 2021. Optimization of mooring systems in the context of an integrated design methodology. Mar. Struct. 75, 102874.

Garrett, D., Chappell, J., Gordon, R., Cao, Y., 2003. Integrated design of risers and moorings. In: Deepwater Mooring Systems: Concepts, Design, Analysis, and Materials, pp. 300–315.

Girón, A.R.C., Corrêa, F.N., Hernández, A.O.V., Jacob, B.P., 2014. An integrated methodology for the design of mooring systems and risers. Mar. Struct. 39, 395–423.

Ja'e, I.A., Ali, M.O.A., Yenduri, A., Nizamani, Z., Nakayama, A., 2022. Optimisation of mooring line parameters for offshore floating structures: a review paper. Ocean Eng. 247, 110644.

Kaucic, M., 2013. A multi-start opposition-based particle swarm optimization algorithm with adaptive velocity for bound constrained global optimization. J. Global Optim. 55 (1), 165–188.

Kim, M., Koo, B., Mercier, R., Ward, E., 2005. Vessel/mooring/riser coupled dynamic analysis of a turret-moored FPSO compared with OTRC experiment. Ocean Eng. 32 (14–15), 1780–1802.

Liang, M., Wang, X., Xu, S., Ding, A., Oct 15 2019. A shallow water mooring system design methodology combining NSGA-II with the vessel-mooring coupled model. Ocean Eng. 190 https://doi.org/10.1016/j.oceaneng.2019.106417. Art no. 106417.

Liu, B., Wang, L., Jin, Y.-H., Tang, F., Huang, D.-X., 2005. Improved particle swarm optimization combined with chaos. Chaos, Solit. Fractals 25 (5), 1261–1271.

Maffra, S.A.R.D.S., Pacheco, M.A.C., de Menezes, I.F. M.g., 2003. Genetic algorithm optimization for mooring systems. Generations 1 (3), 1, 3.

Mehdi, S., Rezvani, A., 2007. Mooring optimization of floating platforms using a genetic algorithm. Ocean Eng. 34 (10), 1413–1421. https://doi.org/10.1016/j.oceaneng.2006.10.005.

Montasir, O., Yenduri, A., Kurian, V., 2019. Mooring system optimisation and effect of different line design variables on motions of truss spar platforms in intact and damaged conditions. China Ocean Eng. 33 (4), 385–397.

Monteiro, B.F., de Pina, A.A., Baioco, J.S., Albrecht, C.H., de Lima, B.S.L.P., Jacob, B.P., 2016. Toward a methodology for the optimal design of mooring systems for floating offshore platforms using evolutionary algorithms. Marine Systems and Ocean Technology 11 (3–4), 55–67. https://doi.org/10.1007/s40868-016-0017-8.

Monteiro, B.D.F., Baioco, J.S., Albrecht, C.H., de Lima, B.S.L.P., Jacob, B.P., 2021. Optimization of mooring systems in the context of an integrated design methodology. Mar. Struct. 75 https://doi.org/10.1016/j.marstruc.2020.102874. Art no. 102874.

Offshore Standard: Position Mooring, 2010. D. N. Veritas.

Piotrowski, A.P., Napiorkowski, J.J., Piotrowska, A.E., 2020. Population size in particle swarm optimization. Swarm Evol. Comput. 58, 100718.
Senra, S.F., Correa, F.N., Jacob, B.P., Mourelle, M.r.M., Masetti, I.a.Q., 2002. Towards the integration of analysis and design of mooring systems and risers: Part I—studies on a semisubmersible platform. Int. Conf. Offshore Mech. Arctic Eng. 36118, 41–48.
Seymour, B., Zhang, H., Wibner, C., 2003. Integrated riser and mooring design for the P-43 and P-48 FPSOs. In: Offshore Technology Conference. Offshore Technology Conference.